Electronic Supplementary Material (ESI) for Sustainable Energy & Fuels.

[Supporting Information]

Boosting Charge Transport in the $BiVO_4$ Photoanode Interface modified with an Aluminum Hydroxide Layer for Solar Water Oxidation

Waka Matsumoto,[a] Takashi Fukushima,[a] Satoshi Heguri,[b] Syuji Fujii,[a]

Shinya Higashimoto [a*]

[a]*Department of Applied Chemistry, Faculty of Engineering, Osaka Institute of Technology, 5-16-1 Omiya, Asahi-ku, Osaka 535-8585, Japan*

[b]*Department of Environmental Engineering, Faculty of Engineering, Osaka Institute of Technology, 5-16-1 Omiya, Asahi-ku, Osaka 535-8585, Japan*

To whom correspondence should be addressed.

Dr. Shinya Higashimoto

Tel: +81-6-6954-4283; fax: +81- 6-6957-2135

E-mail: shinya.higashimoto@oit.ac.jp

Table SI 1 Comparisons of cocatalyst on the $BiVO_4$ photoelectrodes with photocurrent density.

entries	cocatalyst	Electrolytes / pH	Photocurrent / mA cm^{-2} @1.23 V vs. RHE	references
1	Co_3O_4	0.5 M borate buffer / pH 9.5	2.9	[42]
2	FeOOH	0.5 M phosphate buffer / pH 7	3.6	[25]
3	NiOOH	0.5 M phosphate buffer / pH 7	3.3	[25]
4	FeOOH / NiOOH	0.5 M phosphate buffer / pH 7	3.2	[25]
5	NiOOH / FeOOH	0.5 M phosphate buffer / pH 7	4.2	[25]
6	RuCat. (Ru-based molecular catalyst)	0.1 M phosphate buffer / pH 7.1	1.4	[43]
7	CoPi	0.1 M phosphate buffer / pH 7.1	1.3	[43]
8	CoBi	0.5 M borate buffer / pH 9.3	2.0	[44]
9	Fe-g-C_3N_4/$BiVO_4$	0.2 M phosphate buffer / pH 7	2.2	[45]
10	$NiCoO_x$/$BiVO_4$	0.2 M phosphate buffer / pH 7	4.3	[45]
11	G@LDH@$BiVO_4$	0.1 M phosphate buffer / pH 7	2.1	[46]
12	$NiFeO_x$	3.5 % NaOH solution	1.3	[47]
13	NiO_x	0.1 M NaOH+H_2O_2 aqueous solution pH 13	1.9	[48]
14	FeO_x	0.1 M NaOH+H_2O_2 aqueous solution pH 13	1.9	[48]
15	CeO_x	0.1 M NaOH+H_2O_2 aqueous solution pH 13	2.2	[48]
16	$Co_{0.4}Fe_{0.1}Ce_{0.5}O_x$	0.1 M NaOH+H_2O_2 aqueous solution pH 13	2.4	[48]

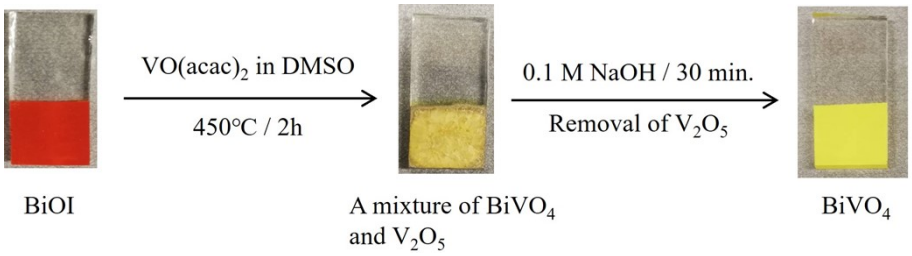

Scheme SI 1 Photo-graphical procedures for fabrication from BiOI to $BiVO_4$.

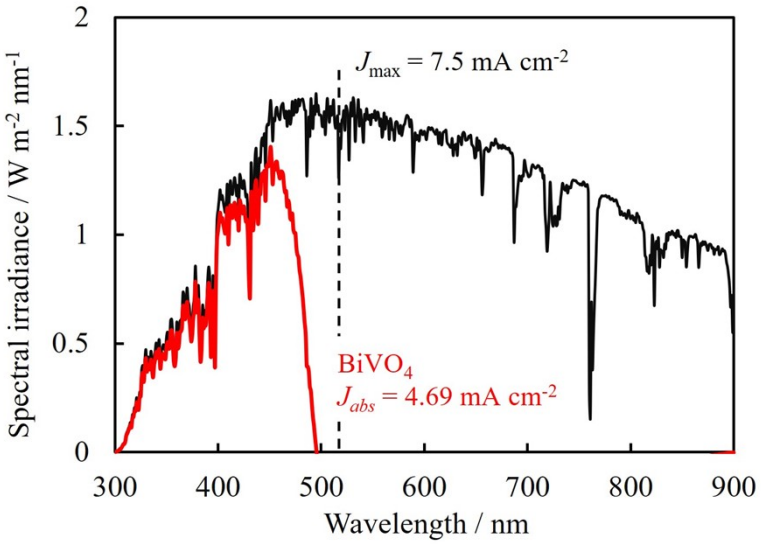

Figure SI 1 Spectral irradiance on the Earth's surface in the standard AM1.5G solar spectrum (black line), and calculated maximum absorption of solar power by $BiVO_4$ (red line).

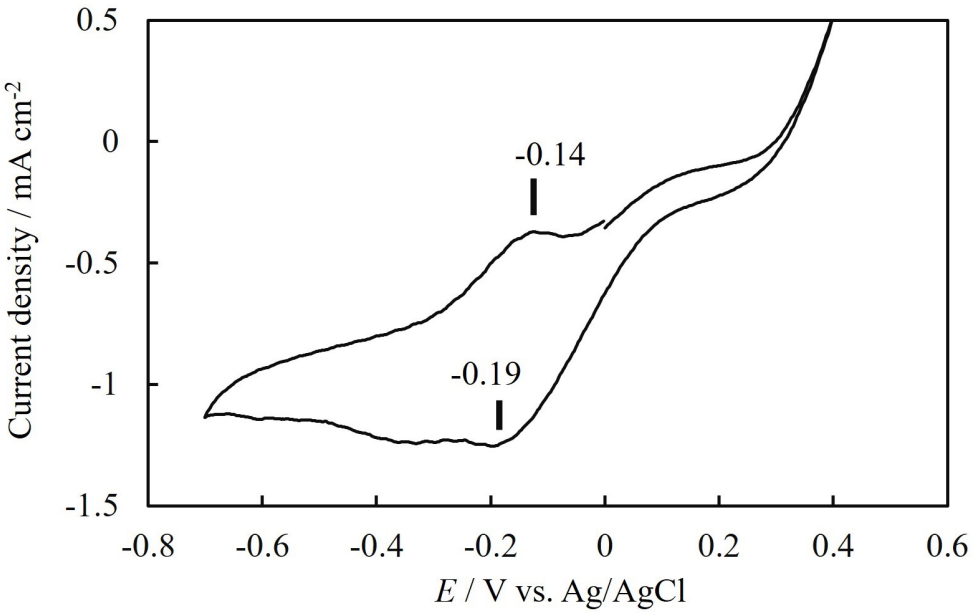

Figure SI 2 Cyclic voltammogram on the FTO substrate in the electrolyte solution involving 0.4 M KI and 0.04 M $Bi(NO_3)_3$ for the electrodeposition of BiOI.

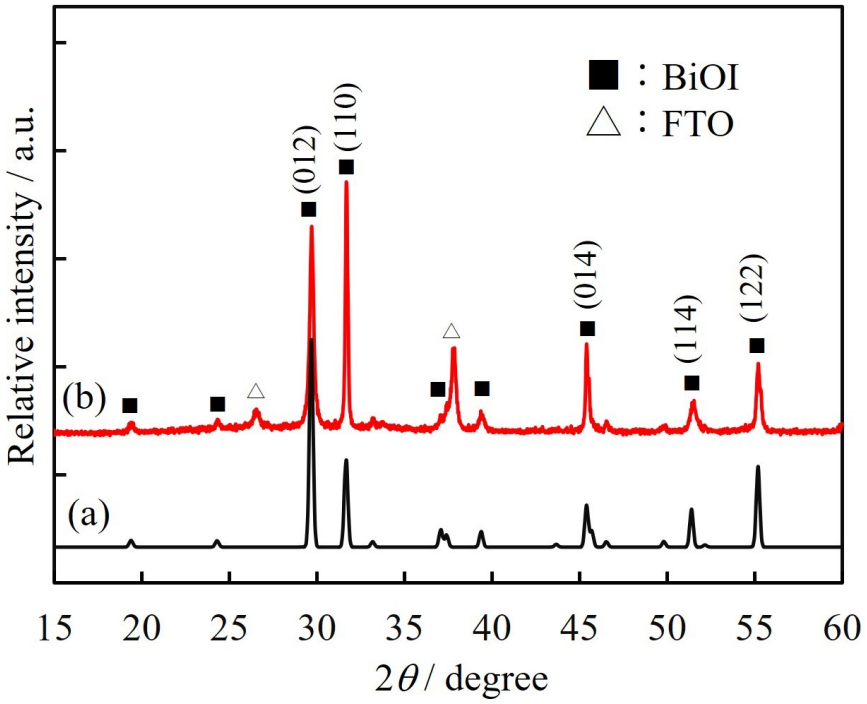

Figure SI 3 XRD patterns of (a) standard powder diffraction pattern of BiOI (JCPDS no. 73-2062), and (b) as-electrodeposited film on FTO.

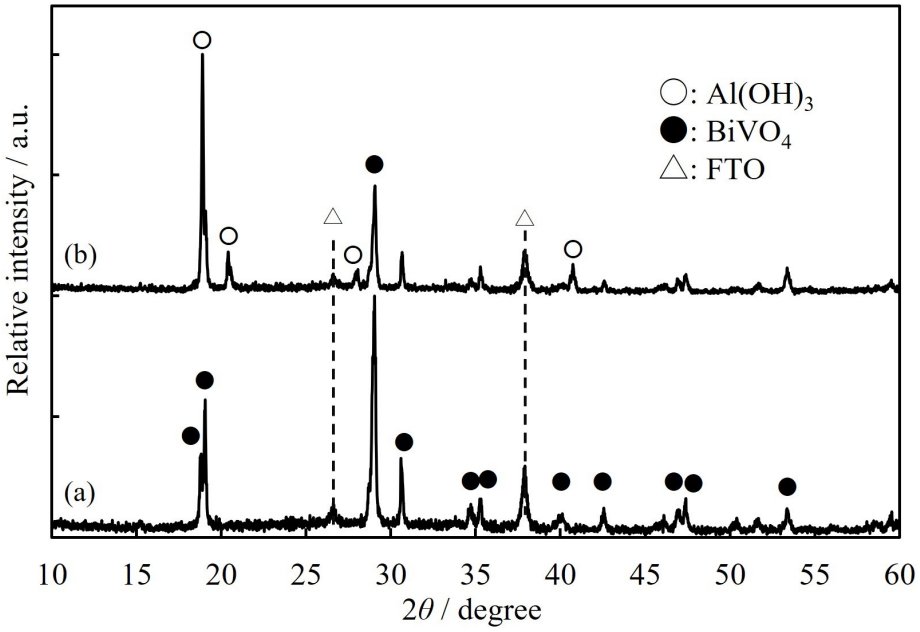

Figure SI 4 XRD patterns of (a) $BiVO_4$ and (b) Al-$BiVO_4$. The Al species on the $BiVO_4$ was deposited in 0.2 M $Al_2(SO_4)_3$ for 19h. $Al(OH)_3$: ICDD 76-1782, $BiVO_4$: pdf 14-133.

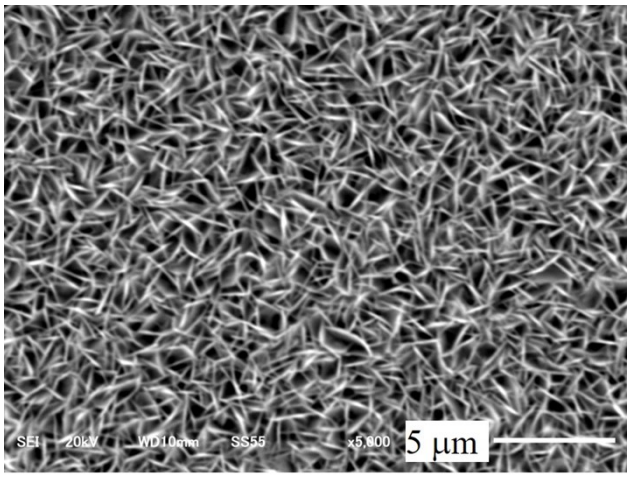

Figure SI 5 SEM image of the BiOI surface.

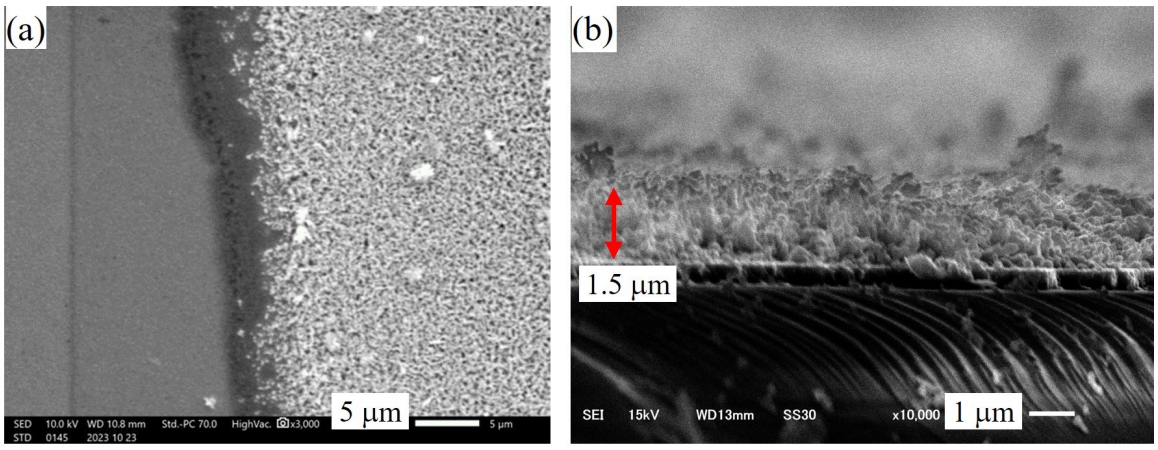

Figure SI 6 SEM images from (a) side and (b) cross-section of the Al-Mo:$BiVO_4$.

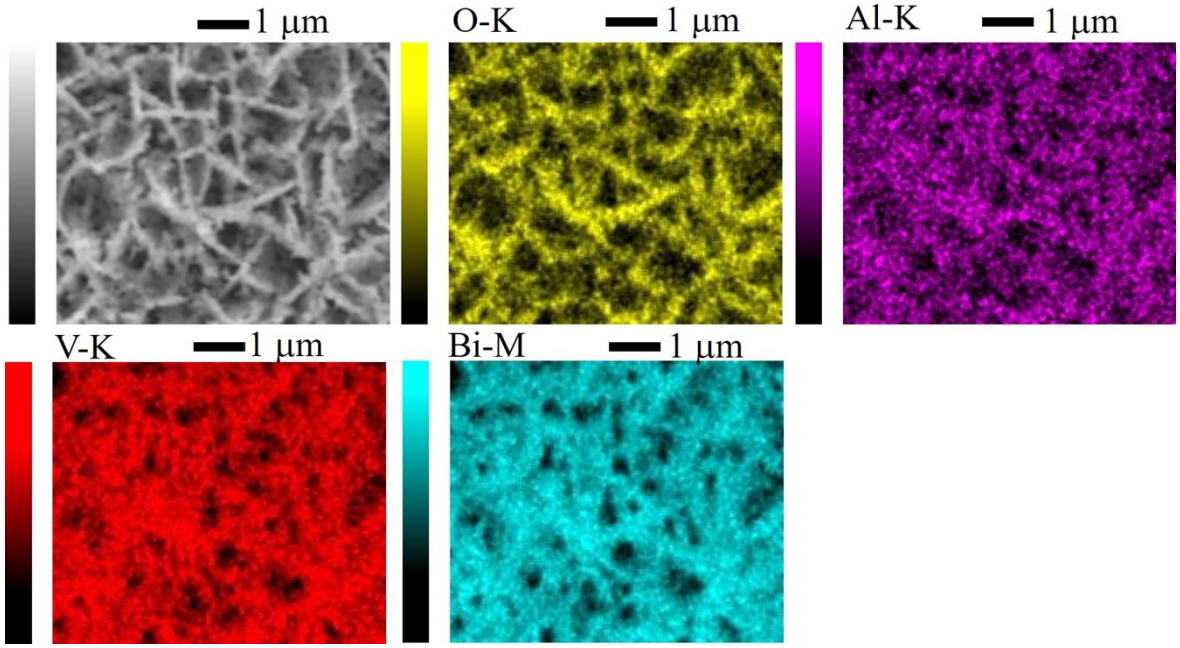

Figure SI 7 EDX mappings for O, Al, V and Bi elements of Al-Mo:$BiVO_4$.

Table SI 2 Atomic compositions of $BiVO_4$, Mo:$BiVO_4$ and Al-Mo:$BiVO_4$ determined by EDX (10 kV). The composition of Sn is derived from the FTO substrate.

	V	Bi	O	Mo	Al	Sn
$BiVO_4$	1	1.30	2.25	ND	-	0.18
Mo-$BiVO_4$	1	1.27	2.25	ND	-	0.22
Al-Mo:$BiVO_4$	1	1.26	2.26	ND	0.018	0.19

Table SI 3 Composite ratios of oxygen species on $BiVO_4$, Mo:$BiVO_4$ and Al-Mo:$BiVO_4$ after deconvolution of XPS O1s peaks

photoelectrodes	component	Energy / eV	ratio / %
$BiVO_4$	C_1	529.6	70.3
	C_2	530.7	29.7
Mo:$BiVO_4$	C_1	529.7	71.9
	C_2	530.7	28.1
Al-Mo:$BiVO_4$	C_1	529.7	33.4
	C_2	530.7	14.8
	C_3	532.0	51.8

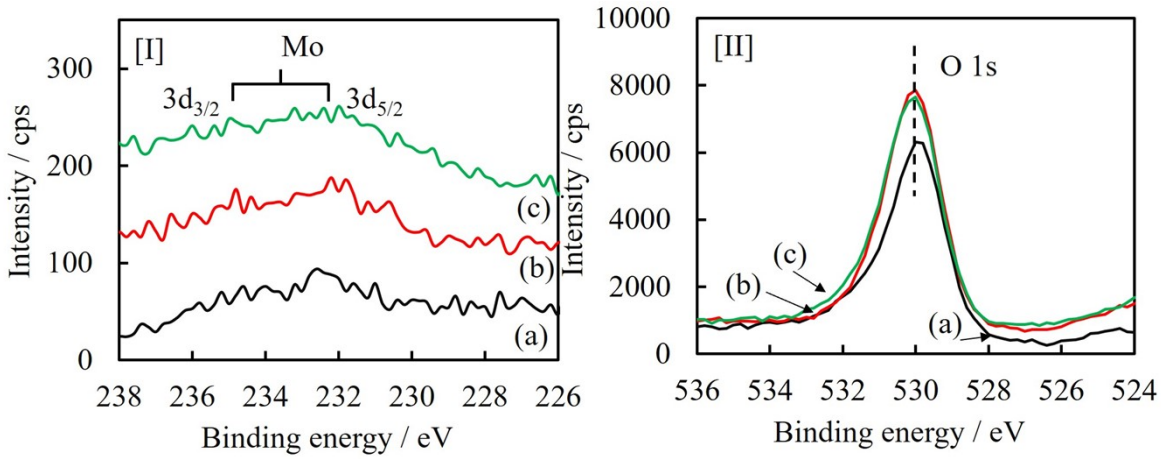

Figure SI 8 Mo [I], O [II] XPS spectra with argon etching of the Mo-$BiVO_4$ photoelectrode surface for (a) 0, (b) 10 and (c) 30s.

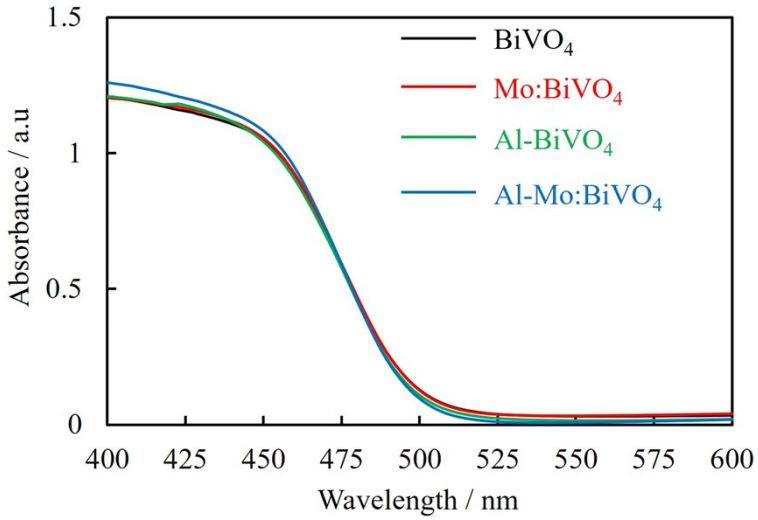

Figure SI 9 UV-Vis spectra of $BiVO_4$, Mo:$BiVO_4$, Al-$BiVO_4$, Al-Mo:$BiVO_4$ photoelectrodes.

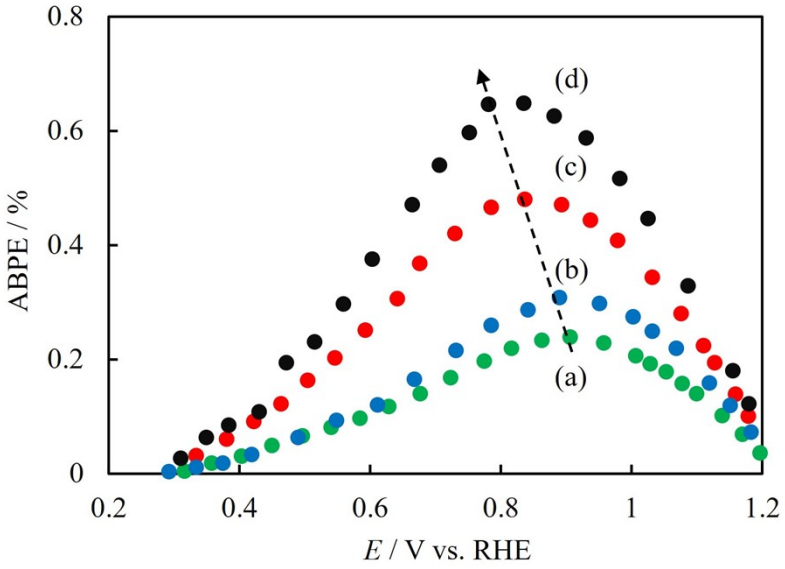

Figure SI 10 ABPE on the (a) $BiVO_4$, (b) Mo:$BiVO_4$, (c) Al-$BiVO_4$, (d) Al-Mo:$BiVO_4$ in 0.5 M borate buffer solution (pH 9.5) under illumination from AM 1.5G solar simulator.

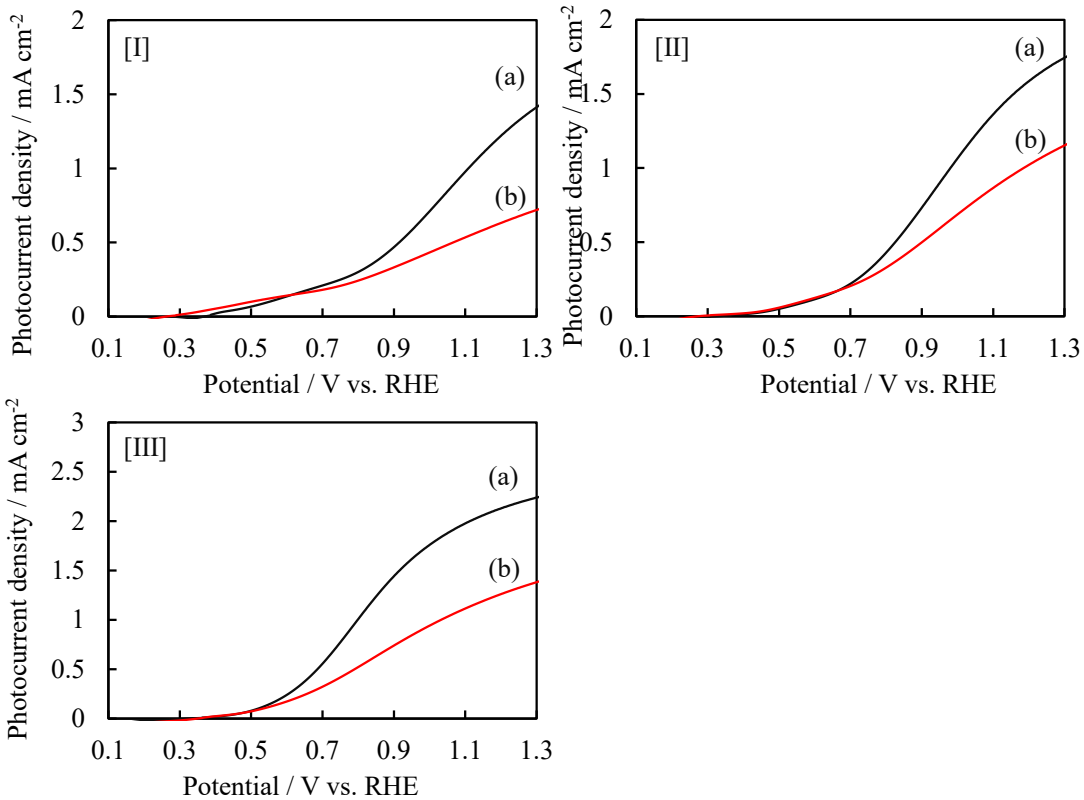

Figure SI 11 I_{ph}-V curves on [I] $BiVO_4$, [II] Mo:$BiVO_4$, [III] Al-Mo:$BiVO_4$ in 0.5 M borate buffer solution (pH 9.5) through back (a) and front (b) irradiation from AM 1.5 solar simulator.

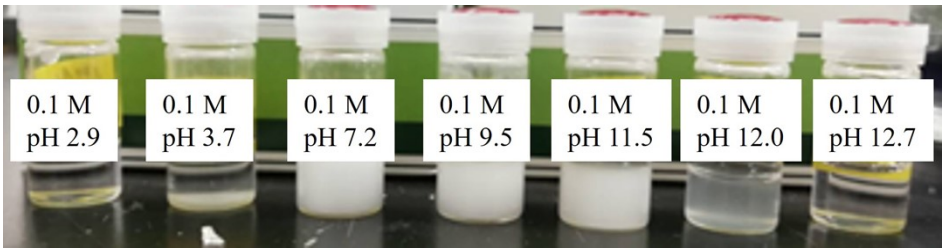

Figure SI 12 Photo-images of 0.1 M $Al_2(SO_4)_3$ as a function of pH.

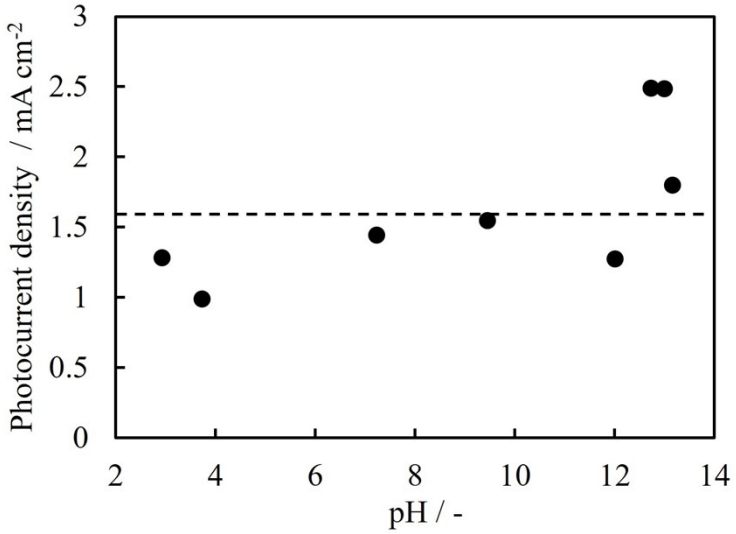

Figure SI 13 Effect of pH of $Al_2(SO_4)_3$ solutions for preparation of the Al-Mo:$BiVO_4$ photoelectrodes on the photocurrent density in 0.5 M borate buffer solutions (pH 9.5) under illumination from AM 1.5G solar simulator. Photoelectrodes were immersed in solutions with different pH for 6 h at 298 K.

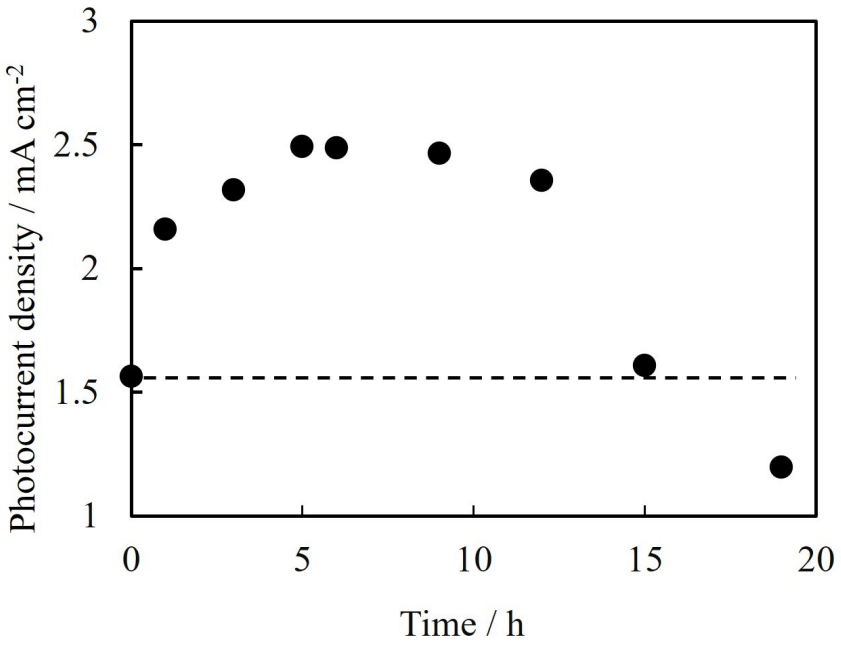

Figure SI 14 Effect of deposition time of Al^{3+} ions for preparation of the Al-Mo:$BiVO_4$ photoelectrode on the photocurrent density in 0.5 M borate buffer solution (pH 7) under illumination from AM 1.5G solar simulator. The photoelectrodes were immersed in solutions (pH 12.7) in 0.1 M $Al_2(SO_4)_3$ aq. at 298 K.

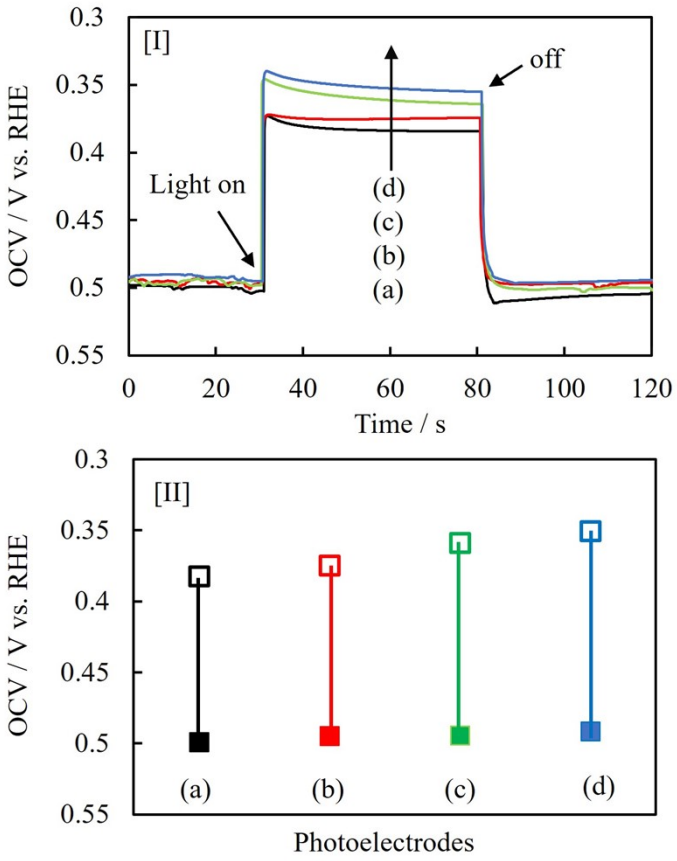

Figure SI 15 Change of photo-charging potentials [I] and schematics of open circuit voltages [II] on (a) $BiVO_4$, (b) Mo:$BiVO_4$, (c) Al-$BiVO_4$, (d) Al-Mo:$BiVO_4$ in 0.5 M borate buffer solution (pH 9.5) under illumination from AM 1.5G solar simulator.

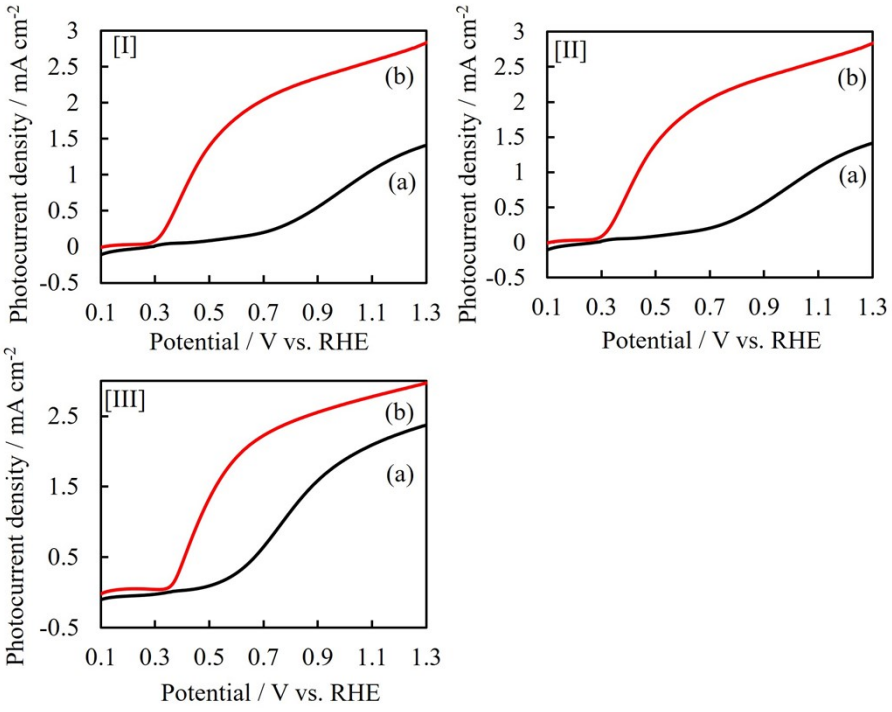

Figure SI 16 I_{ph}-V curves on [I] $BiVO_4$, [II] Mo:$BiVO_4$, [III] Al-Mo:$BiVO_4$ in 0.5 M borate buffer solution (pH 9.5) in the absence (a) and presence (b) of 0.2 M Na_2SO_3 under illumination from AM 1.5G solar simulator.

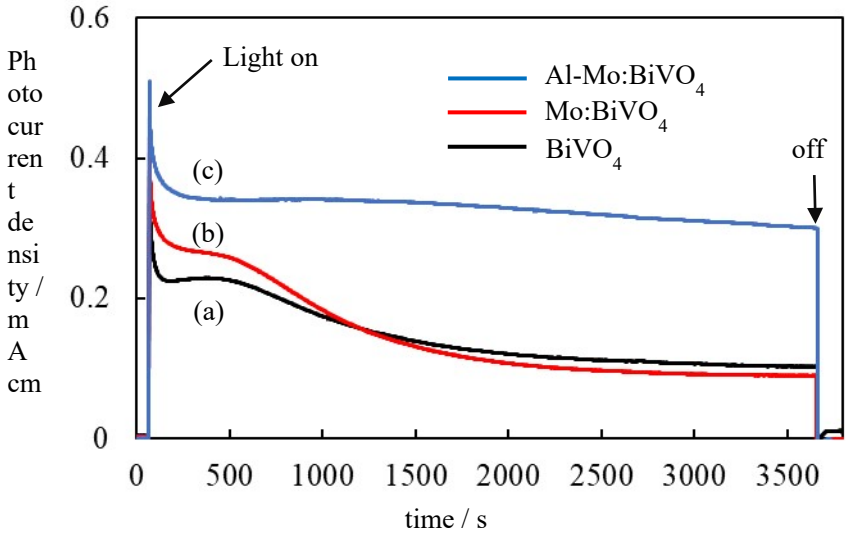

Figure SI 17 Stability of photocurrent density on (a) $BiVO_4$, (b) Mo:$BiVO_4$, and (c) Al-Mo:$BiVO_4$ at +0.8 V vs. RHE in 0.5 M borate buffer solution (pH 9.5) under photo-irradiation from AM 1.5 solar simulator.

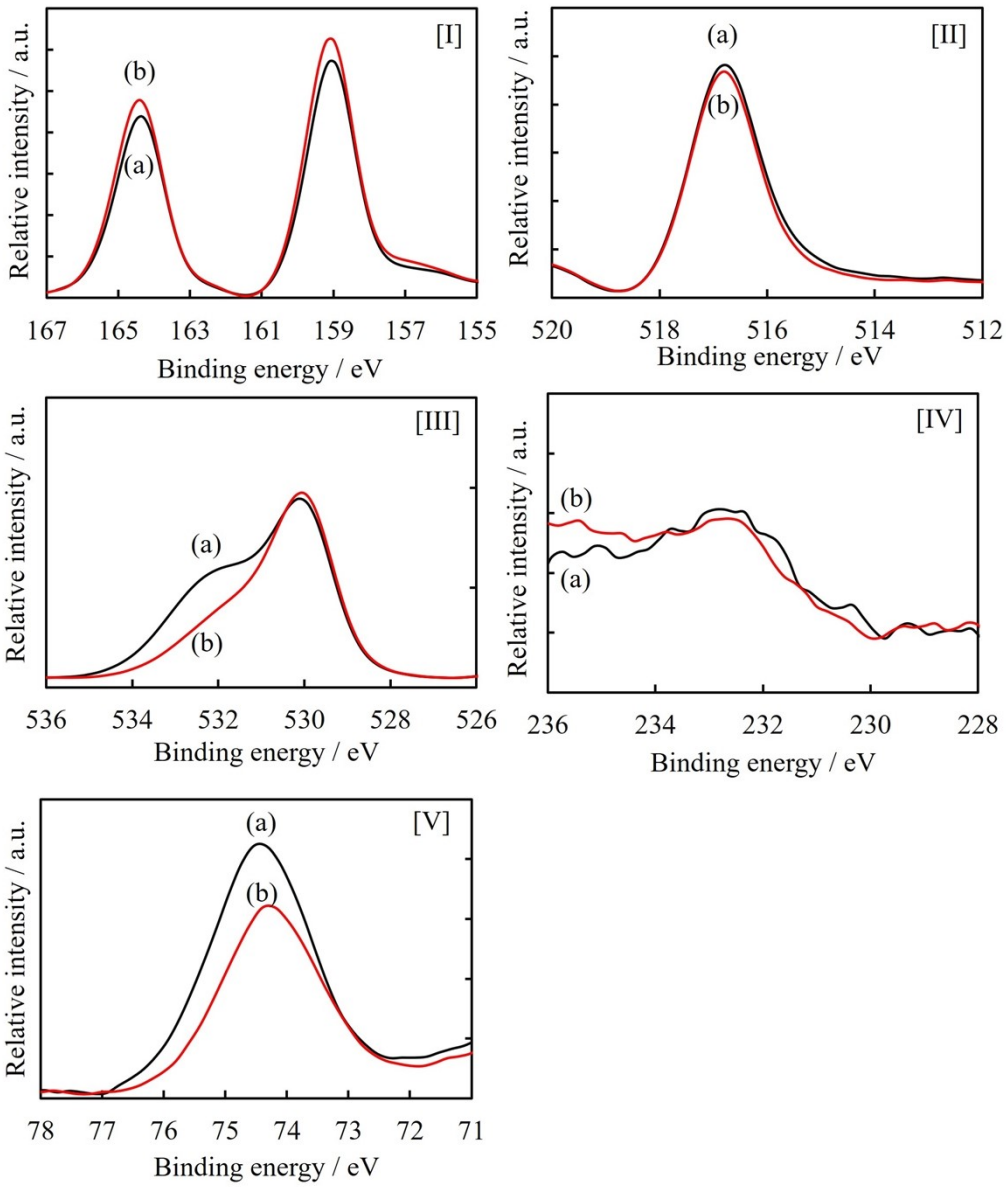

Figure SI 18 Changes in various XPS spectra of [I] Bi, [II] V, [III] O, [IV] Mo, [V] Al on the Al-Mo:$BiVO_4$ photoelectrode before (a) and after (b) photo-irradiation. Photoelectrode was biased at +0.8 V vs. RHE in 0.5 M borate buffer solution (pH 9.5) under photo-irradiation from AM 1.5 solar simulator for 1h.

(a)

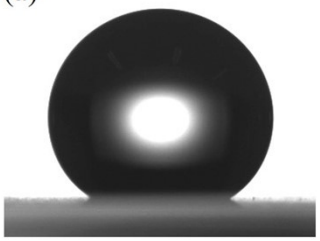

Number of measurements	contact angle / degree
1	149.7
2	138.3
3	142.4
Avg.	143.5

(b)

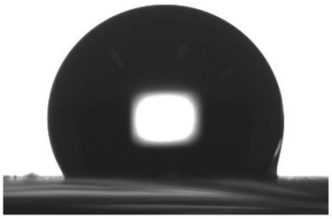

Number of measurements	contact angle / degree
1	119.7
2	124.2
3	121.1
Avg.	121.7

Figure SI 19 Photographs of photoelectrode: (a) $BiVO_4$, (b) Al-$BiVO_4$ contacted with water droplets.